Robust Non-Linear Controller Design for DC-DC Buck Converter via Modified Back-Stepping Methodology

Okba Boutebba[1, 2, *], Samia Semcheddine[1], Fateh Krim[1], Billel Talbi[1], Alberto Reatti[2], Fabio Corti[2]

[1]*Department of Electronics, Laboratory of Power Electronics and Industrial Control (LEPCI), University of Setif-1, Setif, 1900, Algeria*

[2]*Department of Information Engineering, DINFO, Universita degli Studi di Firenze, Via di Santa Marta 3, 50139, Florence, Italy*

boutebbaokba@univ-setif.dz

***Abstract*—This paper introduces two improved control algorithms for DC-DC converters. The first one is called "Non-Adaptive Modified Back-Stepping Control" (M-BSC) and the second one is called "Adaptive Modified Back-Stepping Control" (AM-BSC). Both the proposed control schemes allow one to increase the robustness to load and input voltage variations and make the DC-DC converter less sensitive to disturbances concerning the control algorithms available in the literature. The control aims to keep the output voltage at the desired value despite any changes that may occur during its operation. As a case study, the proposed control techniques have been applied to a DC-DC Buck converter. To validate the theoretical results and evaluate the performance of the proposed control algorithms, numerical simulations with four different scenarios have been analyzed: nominal operating conditions, load variations, output voltage tracking, and input voltage variations. The simulation results highlight the good performance of the proposed control algorithms compared to other classical algorithms, improving both the stationary error and the response time.**

***Index Terms*—DC-DC converter; Modified back-stepping control; Adaptive modified back-stepping control; Robustness.**

I. INTRODUCTION

One of the most important properties of a DC-DC converter is its dynamic response to variations under a wide range of operating conditions. Usually, the output voltage must be regulated against the input voltage and load variations. For this reason, several control strategies have been developed. Linear controllers represent the most commonly used solution due to their simplicity and ease of design. These types of control are also known as Proportional-Integrative-Derivative (PID) controllers [1], [2]. The PID design is based on the linearization of the power converter in correspondence with a particular operating condition. Since power converters are made up of non-linear elements, such as Metal-Oxide-Semiconductor Field-Effect Transistors (MOSFETs), this approximation leads to a degradation of the control performance when the power converter operates far from the linearization point. For this reason, PID controllers can be a powerful solution around a fixed operating point assuming low disturbances, but cannot be suitable for those applications where high accuracy and dynamic performance are required under a wide operating condition range. This inaccuracy can lead to unstable operation of the power converter once the control loop is closed. As a solution to instability problems and ineffective performance, several robust non-linear controllers have been proposed, such as predictive control [3], [4], intelligent control [5], [6], Sliding Mode Control (SMC) [7]–[9], and Back-Stepping (BS) [10]–[13]. These controls provide a fast transient response time and robustness.

In [9], the singular problem of the Terminal Sliding Mode Control (TSMC) has been removed which increases the robustness and reduces the transient response time. The major drawback is the possibility to regulate only the voltage. In addition, the current through the inductor under different uncertainties has not been investigated.

In [14] and [15], Synergetic Control (SC) and Fast Terminal Synergetic Control (FTSC) have been proposed. These strategies are based on the invariance property of the SMC. These controllers have been tested under step load changes, input perturbation, and output voltage variations, showing good performance in voltage regulation in case of uncertainty of system parameters. Anyway, the major drawback of these techniques is the requirement of an accurate system model.

To overcome this problem, a non-linear Adaptive Back-Stepping Control (ABSC) technique has been proposed in [16], [17]. This control allows to achieve the desired control goals whereas ensuring the stability of the entire closed loop system. ABSC incorporates the benefits of both classical Back-Stepping Control (BSC) and adaptive strategies, which are derived from the Lyapunov stability criteria approach to obtain at the same time a robust and self-learning system. The key strength of BSC can be found in

Manuscript received 12 July, 2022; accepted 7 October, 2022.

its systematic and recursive design. In addition to focusing on the asymptotic convergence of the error, it also confirms the convergence of the intermediate variables of the tracking error. Its important advantages include a rapid transient performance, robustness to system-parametric uncertainty, and finally, a superb performance against unmodeled system dynamics and external disturbances.

In [16]–[19], different controllers have been derived based on the BS methodology. In [16], [17], both adaptive and non-adaptive versions of the BS controller have been applied to a DC-DC Buck converter under different modes. The major drawbacks are that the analysis has been performed only through theoretical simulations and that the applied techniques work properly only when the converter parameters are perfectly known, more specifically when the load is constant. However, these BS controllers may nevertheless deliver acceptable behaviour if their design gains are suitably specified.

To mitigate these issues, both Non-Adaptive Modified Back-Stepping Control (M-BSC) and AM-BSC for a DC-DC Buck converter are proposed in this work to increase the robustness voltage control under a wide range of operating conditions and parameters uncertainties. In addition, the proposed approaches reduce the time to reach the equilibrium point and lead to convergence and mitigation of disturbances.

The paper is organized as follows. In Section II, the M-BSC controller for a DC-DC Buck converter is detailed, and its results are compared with classical BSC to show its advantages. In Section III, the AM-BSC controller is detailed, and the simulation results are compared against the M-BSC, BSC, and Proportional Integral (PI) controllers. Finally, the conclusions and possible extensions of the research are presented in this paper.

II. MODIFIED BACK-STEPPING CONTROLLER

A. DC-DC Buck Converter

To evaluate and compare the dynamic performance of the proposed controllers, a Buck converter is investigated as a case study. The electric circuit is shown in Fig. 1.

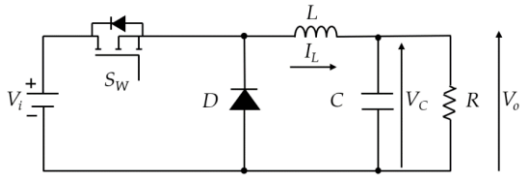

Fig. 1. Topology of the DC-DC Buck power converter.

The Buck converter is made up of a MOSFET S_W, a diode D, an inductor L, a capacitor C, and a load resistance R. The input voltage is V_i whereas the output voltage is V_o.

The assumptions in this work are that the converter is operating in Continuous Conduction Mode (CCM). Depending on operation of the switch S_W, the desired output voltage can be obtained. Generally, the dynamic behaviour of the Buck has two states:

– *State 1*: If S_W ON, the diode D does not conduct and the input V_i acts as the sole source of energy into the Buck converter.

– *State 2*: If S_W OFF, the inductor L and capacitor C release energy to the load via the free-wheeling diode D, and this latter resumes electrical conduction, ensuring the flow of current through the inductor L. Therefore, the stored energy in L drives the load R during the OFF mode of power switch S_W.

The average state-space model describing the voltage and current dynamics of a step-down converter in CCM under two working modes is given by [20], [21]:

$$\dot{x}_1 = -\frac{1}{L}x_2 + d_C\frac{V_i}{L}, \tag{1}$$

$$\dot{x}_2 = \frac{1}{C}x_1 - \frac{1}{RC}x_2, \tag{2}$$

where $x_1 = I_L$ (t) is the inductor current, while $x_2 = V_C$ (t) is the voltage across the output capacitor C.

B. Analytical Design Procedure

By integrating the concept of the classical BS control mechanism presented in [16], [17], the M-BSC is proposed and designed to track the output voltage of a Buck DC-DC converter. The architecture of the M-BSC controller is a recursive process. It involves a clear and systematic construction of both the feedback control law and one of the associated classical Lyapunov functions [22].

The M-BSC generally includes two steps since the Buck DC-DC converter is a 2nd order system. The first concerns the design and identification of the virtual control function, on which acts as an inductance current reference. The control law is designed in the second step.

1. Identification of the virtual control function ζ

To obtain a high performance control and to produce precise tracking and increase robustness to load and input voltage variations and make the DC-DC converter less sensitive to disturbances related to control algorithms available in the literature [16], [17], an integral term is added to the error expression in the M-BSC theory.

The output error signal (e_1) in the M-BS controller can be expressed as follows

$$e_1 = z_1 + \lambda\int z_1\, dt, \tag{3}$$

where $z_1 = x_2 - u_r$, u_r is the output voltage reference, and λ is a positive coefficient.

Our objective is to obtain a new law control as a function of the state variables which satisfies the desired output voltage such as $x_2 = u_r$, and to steer the signal of e_1 to 0, for several operating modes.

Using (2), the result of the error derivative is expressed as

$$\dot{e}_1 = \left(\frac{1}{C}x_1 - \frac{1}{RC}x_2 - \dot{u}_r\right) + \lambda z_1. \tag{4}$$

One of the classical Lyapunov functions to determine the attractiveness and stability conditions is that of quadratic functions of the type

$$V_1 = \frac{1}{2}e_1^2. \tag{5}$$

Both convergence and asymptotic stability (equilibrium point) are achieved if V_1 is definitively positive, radially unbounded, and its derivative $\dot{V}_1$ is negative.

According to (5), the V_1 derivative with respect to time is given by

$$\dot{V}_1 = e_1 \dot{e}_1. \tag{6}$$

The combination of (6) and (4) results in

$$\dot{V}_1 = e_1 \left(\frac{1}{C} x_1 - \frac{1}{RC} x_2 - \dot{u}_r + \lambda z_1 \right). \tag{7}$$

To obtain a negative derivative of Lyapunov function $\left(\dot{V}_1 < 0\right)$, the following condition must be verified

$$\frac{1}{C} x_1 = -k_1 e_1 + \frac{1}{RC} x_2 + \dot{u}_r - \lambda z_1, \tag{8}$$

where k_1 is a constant and positive gain.

Substituting (8) into (7), one obtains the following

$$\dot{V}_1 = -k_1 e_1^2. \tag{9}$$

Finally, the virtual control ζ which acts as an inductance current reference can be expressed from (8) as

$$\xi = -k_1 e_1 + \frac{1}{RC} x_2 + \dot{u}_r - \lambda z_1. \tag{10}$$

2. Identification of the duty cycle d_C

The second error variable is

$$e_2 = \frac{1}{C} x_1 - \xi. \tag{11}$$

By differentiating (11), (4) becomes

$$\dot{e}_1 = \left(\xi - \frac{1}{RC} x_2 - \dot{u}_r + \lambda z_1 \right) + e_2 = -k_1 e_1 + e_2. \tag{12}$$

The second error derivative $\dot{e}_2$ is derived as

$$\dot{e}_2 = -\frac{1}{LC} x_2 + d_C \frac{V_i}{LC} + k_1 \left(e_2 - k_1 e_1 \right) - \\ - \frac{1}{RC^2} x_1 + \frac{1}{\left(RC\right)^2} x_2 - \ddot{u}_r + \lambda \dot{z}_1. \tag{13}$$

The objective here is to achieve the total system stability and convergence of both (e_1, e_2) to zero (equilibrium point in the closed loop). The global Lyapunov is expressed as

$$V_g = \frac{1}{2} e_1^2 + \frac{1}{2} e_2^2. \tag{14}$$

Deriving this one along the time trajectory, one obtains the following

$$\dot{V}_g = -k_1 e_1^2 + e_2 \left(e_1 + \dot{e}_2 \right). \tag{15}$$

Therefore, from (15), $\dot{V}_g$ is definitively negative if

$$e_1 + \dot{e}_2 = -k_2 e_2, \tag{16}$$

where k_2 is a positive constant gain.

By rearranging and solving (16), the final form of the input control-based Buck DC-DC converter control law is determined as follows

$$d_C = \frac{LC}{V_i} \Big[e_1 \left(k_1^2 - 1 \right) - e_2 \left(k_1 + k_2 \right) - \lambda \dot{z}_1 + \\ + \frac{1}{RC^2} x_1 - x_2 \left(\frac{1}{\left(RC\right)^2} - \frac{1}{LC} \right) + \ddot{u}_r \Big]. \tag{17}$$

Proposition 1:

The M-BSC control law (system studied in closed loop) obtained in (17) ensures the global asymptotic stability of the equilibrium point (x_1, x_2, d_C) = (I_d, u_r, D), where:

$$D = \frac{u_r}{V_i}, \tag{18}$$

$$I_d = \frac{u_r}{R}, \tag{19}$$

where I_d, u_r, D are respectively, the desired current, reference voltage, and the control law.

C. Simulation Results

To evaluate the dynamic response of the proposed M-BSC strategy, a numerical simulation has been performed in MATLAB/Simulink®. The values of the Buck converter parameters and the proposed M-BSC gains are summarized in Table I. All components are assumed to be ideal at first instance. Parasitic resistances of the passive components are considered in the simulation as they can influence the system performance [23], [24].

Four different tests have been performed to evaluate the robustness of M-BSC with respect to the conventional BSC.

TABLE I. CONVERTER OPERATING CONDITIONS AND M-BSC GAINS.

Parameter	Value
Nominal Input Voltage V_i	48 V
Nominal Output Voltage V_o	9 V
Operating Frequency f	20 kHz
MOSFET Parasitic resistance r_m	0.1 Ω
Inductor L	1 mH
Inductor Parasitic resistance r_L	0.02 Ω
Output Capacitor C	120 µF
Capacitor Parasitic resistance r_C	0.1 Ω
Nominal Load Resistance R	10 Ω
M-BSC gains: k_1, k_2, λ	1200, 100, 400

Scenario 1: Nominal Operating Conditions

The Buck converter operates under its rated conditions as shown in Table I. An output voltage V_o = 9 V is requested at

the output.

The comparison between M-BSC and BSC under these conditions is shown in Fig. 2. Both the M-BSC and BSC controllers provide the right steady-state output voltage with short response times. Furthermore, the integral action of the proposed M-BSC controller generates a temporary overrun during the transient. M-BSC is characterized by a lower steady-state output voltage ripple than that of the BSC.

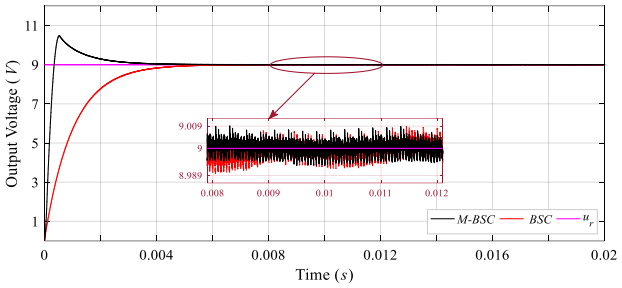

(a)

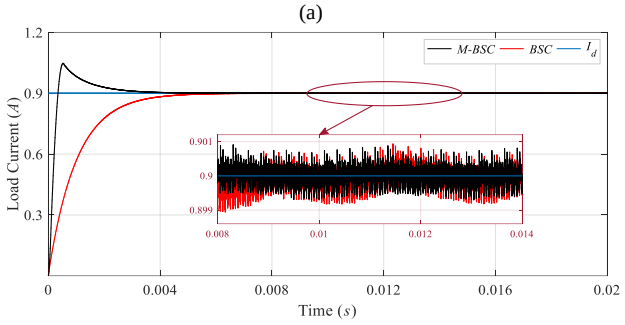

(b)

Fig. 2. Output voltage and current waveforms under nominal operating conditions achieved with M-BSC and BSC (Scenario 1): (a) Output voltage; (b) Load current.

Scenario 2: Load Resistance Variations

The output voltage should be regulated at its nominal value $V_o = 9\ V$ under load variations, which are shown in Table II.

TABLE II. SCENARIO 2: LOAD RESISTANCE VARIATION.

Time Interval	Load Resistance Value R
0 ms–20 ms	10 Ω
20 ms–50 ms	6 Ω
50 ms–80 ms	15 Ω

Figure 3(a) shows that the BS controller completely deviates from the desired output voltage due to the load uncertainties, which present the main drawback of BSC (reacts successfully only when load R is fully known), while the proposed M-BSC has a very fast response and perfectly compensates for the effect due to load changes. Thus, the proposed M-BSC exhibits both effectiveness and robustness against load uncertainties.

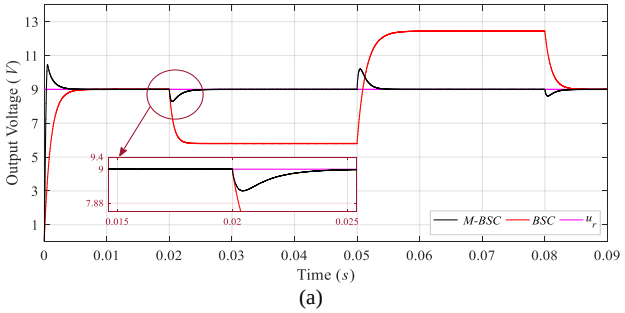

(a)

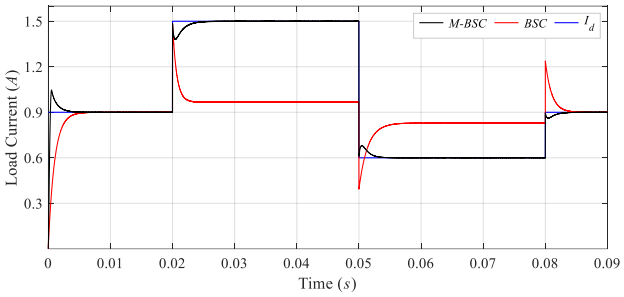

(b)

Fig. 3. Output voltage and current waveforms under load variations achieved with M-BSC and BSC (Scenario 2): (a) Output voltage; (b) Load current.

In addition, it can be seen from the plot of Fig. 3(b) that the current follows the load evolution quite excellent at all times, the latter solely for M-BSC.

Scenario 3: Output Voltage Tracking

In this scenario, the dynamic performance of the controllers in terms of output voltage reference tracking has been evaluated. The desired output voltage over time is summarized in Table III. The simulation results are given in Fig. 4. Both M-BSC and BSC track the output voltage reference u_r promptly, but the M-BSC results in a faster response.

TABLE III. SCENARIO 3: OUTPUT VOLTAGE TRACKING.

Time Interval	Output Voltage V_o
0 ms–20 ms	12 V
20 ms–50 ms	9 V
50 ms–80 ms	5 V

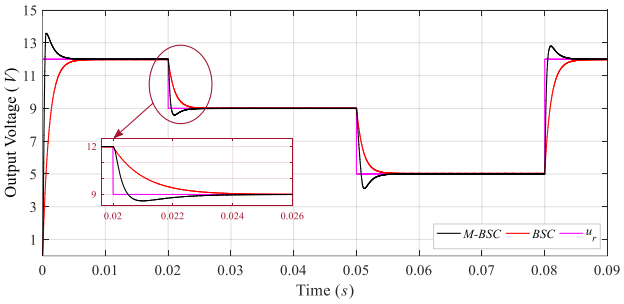

(a)

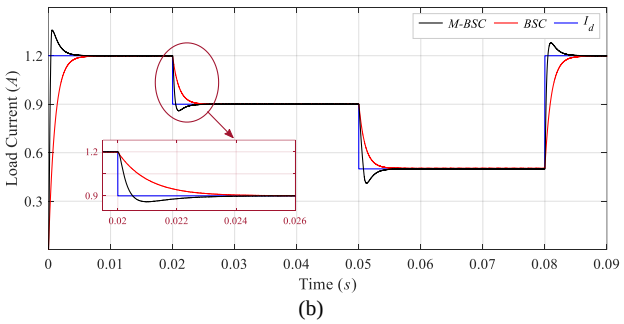

(b)

Fig. 4. Output voltage and current waveforms under output voltage step variations achieved with M-BSC and BSC (Scenario 3): (a) Output voltage; (b) Load current.

Scenario 4: Input Voltage Variations

Finally, the performance of the controllers under input voltage variations is evaluated. The input voltage variations over time are summarized in Table IV.

According to the simulation results, as shown in Fig. 5,

the M-BSC controller allows for a faster compensation of the input voltage variations than BSC. Moreover, the output voltage steady-state errors are lower in the M-BSC than in the BSC. Thus, the M-BSC is more robust and does not present any static error; this is not the case of conventional BSC, which does not follow the reference voltage when an input voltage disturbance occurs, as clearly shown in the zoomed-out view of Fig. 5.

TABLE IV. SCENARIO 4, INPUT VOLTAGE VARIATIONS.

Time Interval	**Input Voltage** V_i
0 ms–20 ms	48 V
20 ms–50 ms	36 V
50 ms–80 ms	60 V

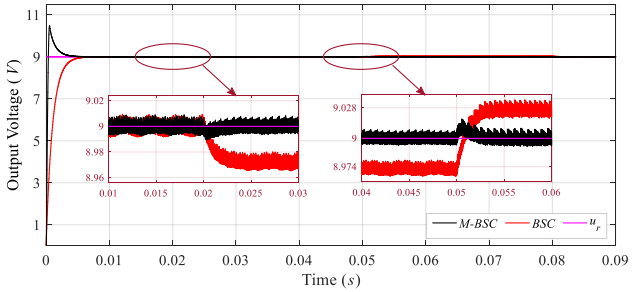

(a)

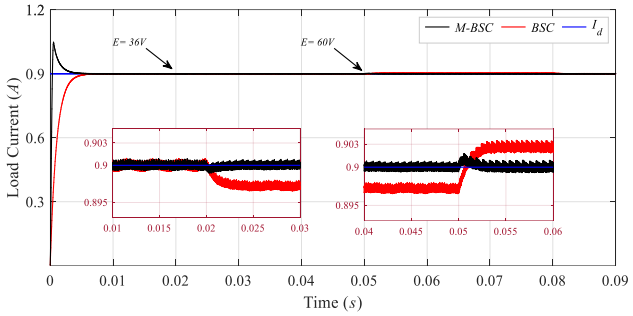

(b)

Fig. 5. Output voltage and current waveforms under input voltage variations achieved with M-BSC and BSC (Scenario 4): (a) Output voltage; (b) Load current.

III. ADAPTIVE MODIFIED BACK-STEPPING CONTROLLER

A. Analytical Design

One of the main important features of a controller is the regulation of the output voltage at a desired value against input voltage and load variations. In the M-BSC design procedure, a constant load operation was assumed in the scenarios considered. However, in most practical applications, the load varies as the power consumption of the circuits, supplied to the power converter, changes.

To overcome this model uncertainty, an Adaptive Modified Back-Stepping Controller (AM-BSC) is proposed. This control strategy allows for an online estimation of the unknown parameter θ, defined as

$$\theta = \frac{1}{R}. \tag{20}$$

The proposed AM-BSC design procedure consists of two steps.

Step 1: Compute the virtual control function ζ.

The derivative error can be expressed as

$$\dot{e}_1 = \frac{1}{C}x_1 - \frac{\theta}{C}x_2 - \dot{u}_r + \lambda z_1. \tag{21}$$

The virtual control ζ, which acts as an inductance current reference, can be expressed as

$$\xi = -k_1 e_1 + \frac{\hat{\theta}}{C}x_2 + \dot{u}_r - \lambda z_1, \tag{22}$$

where k_1 is the AM-BSC design parameter.

The second error (e_2) is defined as

$$e_2 = \frac{1}{C}x_1 - \xi. \tag{23}$$

Substituting (23) and (22) into (21), yields

$$\dot{e}_1 = e_2 - k_1 e_1 - \frac{\tilde{\theta}}{C}x_2, \tag{24}$$

where $\tilde{\theta} = \theta - \hat{\theta}$ is the estimation error.

Step 2: Compute the final control function d_C.

The derivative of e_2 is

$$\dot{e}_2 = \frac{1}{C}\dot{x}_1 - \dot{\xi}. \tag{25}$$

From (22), we obtain the following

$$\dot{\xi} = -k_1 e_2 + k_1^2 e_1 + k_1\frac{\tilde{\theta}}{C}x_2 + \frac{1}{C}\dot{\hat{\theta}}x_2 + \\ + \frac{\hat{\theta}}{C^2}\left(x_1 - \theta x_2\right) + \ddot{u}_r - \lambda\dot{z}_1. \tag{26}$$

Substituting (1) and (26) into (25), it yields the following

$$\dot{e}_2 = -\frac{1}{LC}x_2 + d_C\frac{V_i}{LC} + k_1 e_2 - k_1^2 e_1 - \ddot{u}_r + \lambda\dot{z}_1 - \\ - k_1\frac{\tilde{\theta}}{C}x_2 - \frac{1}{C}\dot{\hat{\theta}}x_2 - \frac{\hat{\theta}}{C^2}\left(x_1 - \theta x_2\right). \tag{27}$$

Now, the objective based to conclude both the final control d_C and the adaptation law $\hat{\theta}$, which allows the system to stabilize (e_1, e_2, $\tilde{\theta}$), in a closed loop operation, is based on the global Lyapunov function

$$V_g = \frac{1}{2}e_1^2 + \frac{1}{2}e_2^2 + \frac{1}{2\gamma}\tilde{\theta}^2, \tag{28}$$

where $\gamma > 0$ is the adaptation gain.

The derivative of V_g with respect to time is given by

$$\dot{V}_g = e_1\dot{e}_1 + e_2\dot{e}_2 + \frac{1}{\gamma}\dot{\tilde{\theta}}\tilde{\theta}. \tag{29}$$

Substitution of (24) and (27) into (29), it yields

$$\dot{V}_g = -k_1 e_1^2 - k_2 e_2^2 + \\ + e_2\left[e_2 - \frac{1}{LC}x_2 + d_C\frac{V_i}{LC} - x_1\frac{\hat{\theta}}{C^2}\hat{\theta}x_2 + \right. \\ \left. + k_2 e_2 - k_1^2 e_1 + e_2 - \ddot{u}_r + \lambda\dot{z}_1 - \frac{\dot{\hat{\theta}}}{C}x_2\right] + \\ + \tilde{\theta}\left[e_2\left(-k_1\frac{1}{C} + \frac{\hat{\theta}}{C^2}\right)x_2 - \frac{x_2}{C}e_1 - \frac{\dot{\hat{\theta}}}{\gamma}\right]. \quad (30)$$

It can be seen from this equation that, to ensure the overall asymptotic stability of the system (e_1, e_2, $\tilde{\theta}$), it is enough to cancel the two expressions multiplied by e_2 and $\tilde{\theta}$ into (30). Therefore, the dynamic equation of duty cycle d_C is derived as

$$d_C = \frac{LC}{V_i}\left[e_1\left(k_1^2 - 1\right) - e_2\left(k_1 + k_2\right) + \frac{1}{LC}x_2\right] + \\ + \frac{LC}{V_i}\left[\frac{\dot{\hat{\theta}}}{C}x_2 + \frac{\hat{\theta}}{C^2}\left(x_1 - \hat{\theta}x_2\right) + \ddot{u}_r - \lambda\dot{z}_1\right], \quad (31)$$

where k_2 is the second design parameter.

At the end of this step, the adaptation parameters are obtained as

$$\dot{\hat{\theta}} = x_2\frac{\gamma}{C}\left[e_2\left(-k_1 + \frac{\hat{\theta}}{C}\right) - e_1\right]. \quad (32)$$

Proposition 2:

The AM-BSC control law (system studied in closed loop) obtained in (31) and the adaptation function (32) ensure the global asymptotic stability of the equilibrium point (x_1, x_2, d_C) = ($\hat{I_d}$, u_r, D), where:

$$\hat{I}_d = \hat{\theta}\,u_r, \quad (33)$$

$$D = \frac{u_r}{V_i}. \quad (34)$$

B. Simulation Results

The four scenarios have been used to evaluate the dynamic response of AM-BSC by comparing it against M-BSC, BSC [16], and the conventional PI controller [25].

The gains used to tune the AM-BSC controller are k_1 = 1200, k_2 = 100, λ = 400, and $\gamma = 9^{-4}$.

In Fig. 6, the step response of the four controllers is compared. It can be seen that the proposed AM-BSC allows for a lower settling time and a lower steady-state error with negligible damping.

The dynamic response under load resistance variations is shown in Fig. 7. Both BSC and PI controllers have the worst performance. On the other hand, the proposed AM-BSC allows faster rejection of the disturbance, while maintaining the output voltage close to the nominal value V_o = 9 V. In Fig. 7(b), the current follows the load evolution quite well against the M-BSC controller. The zoomed-out view shows the output voltage and load current before moving back to its reference values. It can be seen that AM-BSC has smooth profiles without any overshoot with improvement in suppression of oscillations, too.

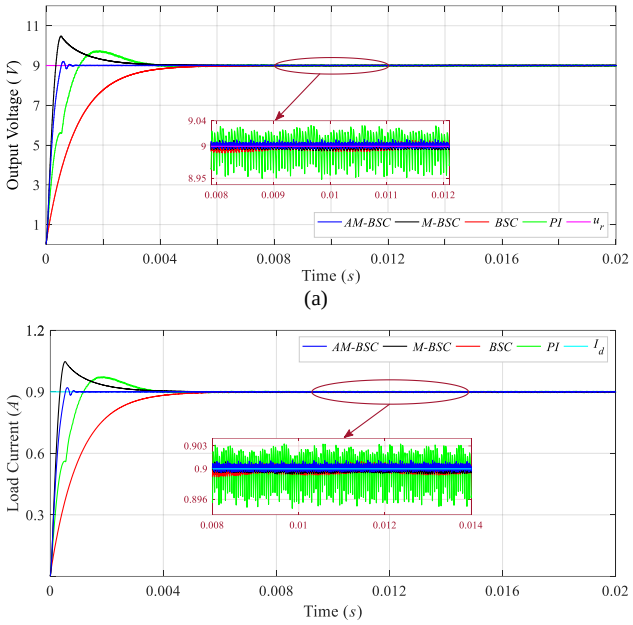

(a)

(b)

Fig. 6. Output voltage and current waveforms under nominal operating conditions with AM-BSC against M-BSC, BSC, and PI: (a) Output voltage; (b) Load current.

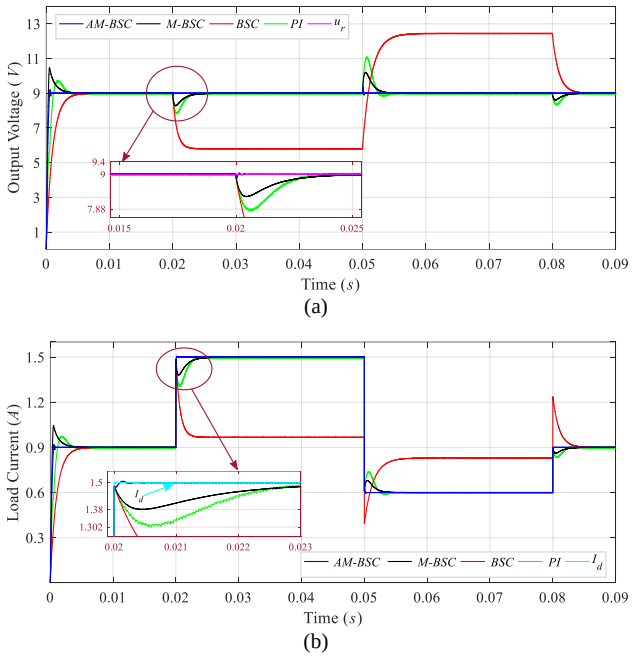

(a)

(b)

Fig. 7. Output voltage and current waveforms under load variations with AM-BSC against M-BSC, BSC, and PI: (a) Output voltage; (b) Load current.

Figure 8(a) shows that the proposed AM-BSC controller allows for a faster tracking of the output voltage and a lower steady-state error compared to M-BSC, BSC, and PI controllers.

In Fig. 9(a), the behaviour of different control strategies has been evaluated for different input voltage variations. In this scenario, the results obtained demonstrate the satisfactory performances of the two control strategies (M-BSC and AM-BSC) in terms of robustness, stationary error,

and chattering of the system. However, the adaptation applied to the M-BSC reduces the overshoot and is more rapid since the response time is clearly better for the AM-BSC controller than for the M-BSC.

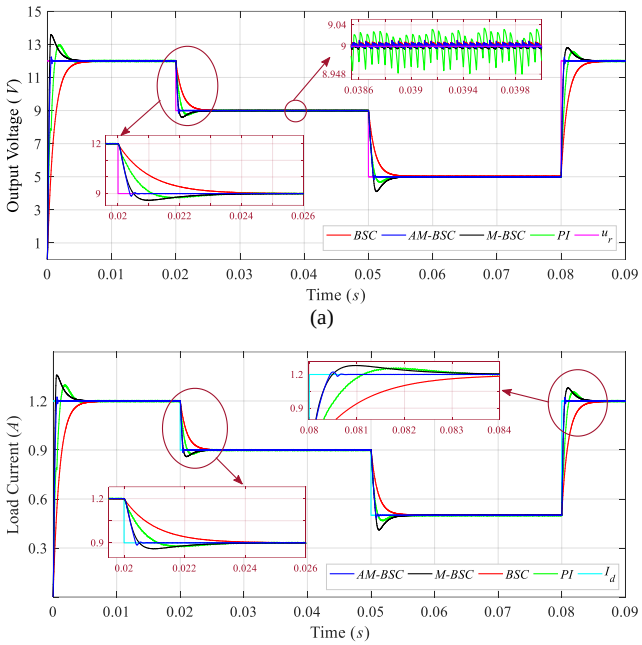

Fig. 8. Output voltage and current waveforms under reference signal variations with AM-BSC against M-BSC, BSC, and PI: (a) Output voltage; (b) Load current.

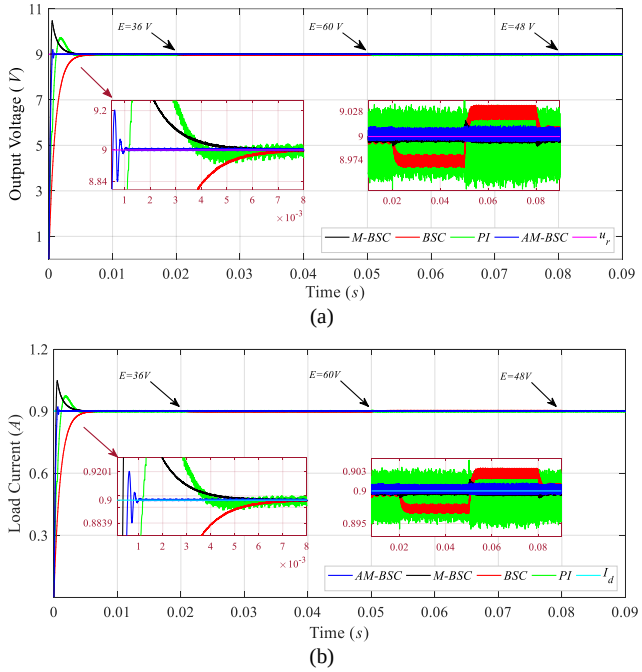

Fig. 9. Output voltage and current waveforms under input voltage step variations with AM-BSC against M-BSC, BSC, and PI: (a) Output voltage; (b) Load current.

Finally, a comparison has been made between the controller responses under the input voltage variation shown in Fig. 10. As shown in Figs. 11(a) and 11(b), the AM-BSC controller reacts with excellent efficiency to input disturbances and promptly compensates for their effect. Moreover, it results in no overshoots, no static errors, and has negligible ripples compared to the M-BSC, BSC, and PI controllers.

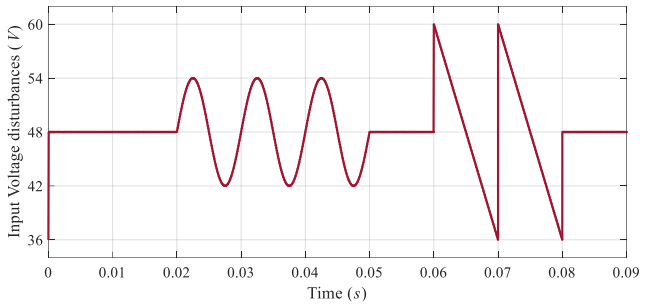

Fig. 10. Waveforms of the input voltage disturbances.

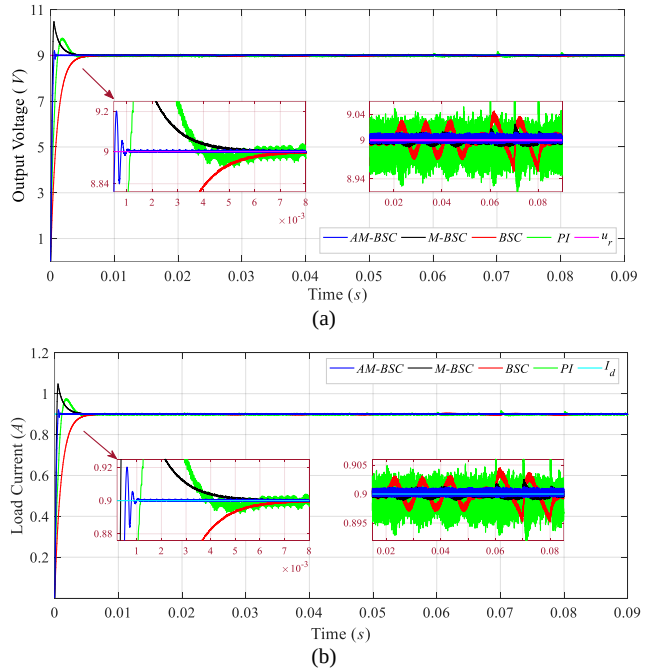

Fig. 11. Output voltage and current waveforms under sine wave and triangle input voltage waveforms with AM-BSC against M-BSC, BSC, and PI: (a) Output voltage; (b) Load current.

IV. CONCLUSIONS

The main goal and impetus for this paper was to propose a robust DC-DC Buck converter controller based on back-stepping control methodology. From the latter, two different control strategies have been performed. The first, called "Modified BSC" (M-BSC), completely overcomes the major inconvenience of conventional back-stepping and performs high robustness against load variation, output voltage tracking, and input voltage variations.

Rendering the development of M-BSC greater robustness with high efficiency, an improved control AM-BSC has been built to achieve the control objective in the presence of unknown load parameters.

To evaluate both the steady-state and dynamic response of the proposed controllers, four different scenarios have been analyzed. The comparative study demonstrated that the proposed M-BSC and AM-BSC control strategy outperforms BSC and PI, in terms of tracking performance with no overshoot, quick dynamic response, shorter rise and settling times, and minimal production tracking error.

In addition to the research presented in this paper, some of the future studies suggested are summarized as follows:

– Perform experimental tests;

– Integrate both converter and algorithm into a photovoltaic chain with Maximum Power Point Tracking (MPPT) control to extract the global maximum power point;

– Fabrication of the control circuit board.

CONFLICTS OF INTEREST

The authors declare that they have no conflicts of interest.

REFERENCES

[1] R. W. Erickson and D. Maksimovic, *Fundamentals of Power Electronics*. Springer, 2001, chs. 8, 9, pp. 265–375. DOI: 10.1007/b100747.

[2] M. He and J. Xu, "Nonlinear PID in digital controlled buck converters", in *Proc. of APEC 07 - Twenty-Second Annual IEEE Applied Power Electronics Conference and Exposition*, 2007, pp. 1461–1465. DOI: 10.1109/APEX.2007.357709.

[3] Q. Xu, Y. Yan, C. Zhang, T. Dragicevic, and F. Blaabjerg, "An offset-free composite model predictive control strategy for DC/DC buck converter feeding constant power loads", *IEEE Transactions on Power Electronics*, vol. 35, no 5, pp. 5331–5342, 2020. DOI: 10.1109/TPEL.2019.2941714.

[4] S. Saadatmand, P. Shamsi, and M. Ferdowsi, "The voltage regulation of a buck converter using a neural network predictive controller", in *Proc. of 2020 IEEE Texas Power and Energy Conference (TPEC)*, 2020, pp. 1–6. DOI: 10.1109/TPEC48276.2020.9042588.

[5] O. Boutebba, A. Laudani, G. M. Lozito, F. Corti, A. Reatti, and S. Semcheddine, "A neural adaptive assisted backstepping controller for MPPT in photovoltaic applications", in *Proc. of 2020 IEEE International Conference on Environment and Electrical Engineering and 2020 IEEE Industrial and Commercial Power Systems Europe (EEEIC/I&CPS Europe)*, 2020, pp. 1–6. DOI: 10.1109/EEEIC/ICPSEurope49358.2020.9160518.

[6] X. Shen, T. Xie, and T. Wang, "A fuzzy adaptative backstepping control strategy for marine current turbine under disturbances and uncertainties", *Energies*, vol. 13, no. 24, p. 6550, 2020. DOI: 10.3390/en13246550.

[7] S. K. Pandey, S. L. Patil, D. Ginoya, U. M. Chaskar, and S. B. Phadke, "Robust control of mismatched buck DC–DC converters by PWM-based sliding mode control schemes", *Control Engineering Practice*, vol. 84, pp. 183–193, 2019. DOI: 10.1016/j.conengprac.2018.11.010.

[8] Z. Wang, S. Li, and Q. Li, "Discrete-time fast terminal sliding mode control design for DC–DC buck converters with mismatched disturbances", *IEEE Transactions on Industrial Informatics*, vol. 16, no. 2, pp. 1204–1213, Feb. 2020. DOI: 10.1109/TII.2019.2937878.

[9] C.-S. Chiu and C.-T. Shen, "Finite-time control of DC–DC buck converters via integral terminal sliding modes", *International Journal of Electronics*, vol. 99, no. 5, pp. 643–655, 2012. DOI: 10.1080/00207217.2011.643493.

[10] H. Shen, J. Iorio, and N. Li, "Sliding mode control in backstepping framework for a class of nonlinear systems", *Journal of Marine Science and Engineering*, vol. 7, no. 12, p. 452, 2019. DOI: 10.3390/jmse7120452.

[11] R. Khan, L. Khan, S. Ullah, I. Sami, and J.-S. Ro, "Backstepping based super-twisting sliding mode MPPT control with differential flatness oriented observer design for photovoltaic system", *Electronics*, vol. 9, no. 9, p. 1543, 2020. DOI: 10.3390/electronics9091543.

[12] O. Boutebba, S. Semcheddine, F. Krim, F. Corti, A. Reatti, and F. Grasso, "A nonlinear back-stepping controller of DC-DC non-inverting buck-boost converter for maximizing photovoltaic power extraction", in *Proc. of 2020 IEEE International Conference on Environment and Electrical Engineering and 2020 IEEE Industrial and Commercial Power Systems Europe (EEEIC/I&CPS Europe)*, 2020, pp. 1–6. DOI: 10.1109/EEEIC/ICPSEurope49358.2020.9160634.

[13] O. Boutebba, S. Semcheddine, F. Krim, and B. Talbi, "Design of a backstepping-controlled boost converter for MPPT in PV chains", in *Proc. of 2019 International Conference on Advanced Electrical Engineering (ICAEE)*, 2019, pp. 1–7. DOI: 10.1109/ICAEE47123.2019.9014748.

[14] N. Zerroug, M. N. Harmas, S. Benaggoune, Z. Bouchama, and K. Zehar, "DSP-based implementation of fast terminal synergetic control for a DC–DC Buck converter", *Journal of the Franklin Institute*, vol. 355, no. 5, pp. 2329–2343, 2018. DOI: 10.1016/j.jfranklin.2018.01.004.

[15] Z. Bouchama, A. Khatir, S. Benaggoune, and M. N. Harmas, "Design and experimental validation of an intelligent controller for DC–DC buck converters", *Journal of the Franklin Institute*, vol. 357, no. 15, pp. 10353–10366, Oct. 2020. DOI: 10.1016/j.jfranklin.2020.08.011.

[16] O. Boutebba, S. Semcheddine, F. Krim, and B. Talbi, "Adaptive nonlinear controller design for DC-DC buck converter via backstepping methodology", in *Proc. of 2019 International Conference on Advanced Electrical Engineering (ICAEE)*, 2019, pp. 1–7. DOI: 10.1109/ICAEE47123.2019.9014825.

[17] H. El Fadil, F. Giri, M. Haloua, and H. Ouadi, "Nonlinear and adaptive control of buck power converters", in *Proc. of 42nd IEEE International Conference on Decision and Control (IEEE Cat. No. 03CH37475)*, 2003, pp. 4475–4480. DOI: 10.1109/CDC.2003.1272244.

[18] H. El Fadil and F. Giri, "Backstepping based control of PWM DC-DC boost power converters", in *Proc. of 2007 IEEE International Symposium on Industrial Electronics*, 2007, pp. 395–400. DOI: 10.1109/ISIE.2007.4374630.

[19] Y. Massaoudi, D. Elleuch, J. P. Gaubert, D. Mehdi, and T. Damak, "A new backstepping sliding mode controller applied to a DC-DC boost converter", *International Journal of Power Electronics and Drive Systems*, vol. 7, no. 3, pp. 759–768, 2016. DOI: 10.11591/ijpeds.v7.i3.pp759-768.

[20] T. K. Nizami and C. Mahanta, "An intelligent adaptive control of DC–DC buck converters", *Journal of the Franklin Institute*, vol. 353, no. 12, pp. 2588–2613, 2016. DOI: 10.1016/j.jfranklin.2016.04.008.

[21] T. K. Nizami, A. Chakravarty, and C. Mahanta, "Time bound online uncertainty estimation based adaptive control design for DC–DC buck converters with experimental validation", *IFAC Journal of Systems and Control*, vol. 15, art. 100127, 2021. DOI: 10.1016/j.ifacsc.2020.100127.

[22] J. Wang, D. Bo, X. Ma, Y. Zhang, Z. Li, and Q. Miao, "Adaptive back-stepping control for a permanent magnet synchronous generator wind energy conversion system", *International Journal of Hydrogen Energy*, vol. 44, no 5, pp. 3240–3249, 2019. DOI: 10.1016/j.ijhydene.2018.12.023.

[23] A. Reatti, F. Corti, A. Tesi, A. Torlai, and M. K. Kazimierczuk, "Effect of parasitic components on dynamic performance of power stages of DC-DC PWM buck and boost converters in CCM", in *Proc. of 2019 IEEE International Symposium on Circuits and Systems (ISCAS)*, 2019, pp. 1–5. DOI: 10.1109/ISCAS.2019.8702520.

[24] E. Locorotondo, L. Pugi, F. Corti, L. Becchi, and F. Grasso, "Analytical model of power MOSFET switching losses due to parasitic components", in *Proc. of 2019 IEEE 5th International forum on Research and Technology for Society and Industry (RTSI)*, 2019, pp. 331–336. DOI: 10.1109/RTSI.2019.8895562.

[25] K. M. Tsang and W. L. Chan, "Cascade controller for DC/DC buck convertor", *Electric Power Applications*, vol. 152, no. 4, pp. 827–831, 2005. DOI: 10.1049/ip-epa:20045198.

This article is an open access article distributed under the terms and conditions of the Creative Commons Attribution 4.0 (CC BY 4.0) license (http://creativecommons.org/licenses/by/4.0/).